SLAC-PUB-1434
(T/E)
May 1974

HADRON PRODUCTION IN ELECTRON-ELECTRON SCATTERING*

Min-Shih Chen

Stanford Linear Accelerator Center
Stanford University, Stanford, California 94305

ABSTRACT

The total and single-hadron inclusive cross sections and energy, momentum, and multiplicity distributions from the two photon process in electron-electron scattering are estimated from the photon-hadron analogy and Regge behavior. Corrections to this estimation and the possible relationships between the electron-electron and electron-positron cross sections are discussed.

(Submitted to Phys. Rev.)

* Work supported by the U.S. Atomic Energy Commission.

There has been extensive discussion on the production of various exclusive final states in electron-electron (e^-e^-) scattering via two photon process[1] but the inclusive features of hadron distributions in this reaction, such as the average multiplicity, single particle spectra, etc., have hardly received as much attention. A better understanding of the latter is important, particularly in view of the unexpected behavior of the hadron production in electron-positron (e^+e^-) scattering.[2] In order to see whether there may be also some unexpected behaviors in e^-e^- scattering, we first have to ask what are expected for the total and inclusive cross sections. A calculation of these cross sections can also serve as estimates of the hadron counting rates in the future e^-e^- experiments and the background in the e^+e^- cross section from the "normal" two photon process.

In the conventional theory of quantum electrodynamics, the hadron production cross section in e^-e^- scattering is dominated by the two photon process

$$e^- + e^- \rightarrow e^- + e^- + \gamma^* + \gamma^* \rightarrow e^- + e^- + \text{hadrons}, \tag{1}$$

as illustrated in Fig. 1a. Since the dominant contribution from this process is restricted in the kinematical region where the masses of both virtual photons are very small, most of the final state electrons are scattered along the beam direction and difficult to detect. Therefore, instead of studying the hadron production the subprocess

$$\gamma^* + \gamma^* \rightarrow \text{hadrons} \tag{2}$$

at fixed total $\gamma^*\gamma^*$ energies, it is more natural to study reaction (1) at fixed e^-e^- center of mass (c.m.) energies with the kinematical variables of the two final state electrons integrated over the allowed phase space. In this manner, we shall discuss the features of the total and inclusive cross sections predicted from the Regge theory, its corrections, and possible deviations from these predictions that may be related to the e^+e^- reactions.

In the equivalent photon approximation,[3-5] the total cross section for reaction (1) can be written as

$$\sigma \simeq \left(\frac{\alpha}{\pi}\right)^2 \left(\ell n \frac{E}{m_e}\right)^2 \frac{1}{E^4} \int \frac{d\omega_1}{\omega_1} \frac{d\omega_2}{\omega_2} \left[E^2 + (E-\omega_1)^2\right]\left[E^2 + (E-\omega_2)^2\right]$$

$$\times \quad \sigma_{\gamma\gamma \to \text{hadrons}} (4\omega_1\omega_2) \qquad \text{(3a)}$$

$$= \left(\frac{\alpha}{\pi}\right)^2 \left(\ell n \frac{E}{m_e}\right)^2 \int_{s_0}^{s} \frac{ds'}{s'} \left[\frac{1}{2}\left(2 + \frac{s'}{s}\right)^2 \ell n \frac{s}{s'} - \left(1 - \frac{s'}{s}\right)\left(3 + \frac{s'}{s}\right)\right]$$

$$\times \quad \sigma_{\gamma\gamma \to \text{hadrons}} (s') \ , \qquad \text{(3b)}$$

where E is beam energy in colliding beam experiments, m_e is the electron rest mass, $s = 4E^2$ is the square of the total invariant mass, ω_1 and ω_2 are the photon energies in the e^-e^- cm frame, $s' = 4\omega_1\omega_2$ is the square of the invariant mass of the hadrons, s_0 is a certain threshold energy for hadron production or cut off in the hadron energy, and $\sigma_{\gamma\gamma \to \text{hadrons}}$ is the total hadron production cross section for $\gamma\gamma$ scattering.

There are at least two possible mechanisms contributing to $\sigma_{\gamma\gamma \to \text{hadrons}}$, namely, the photon-hadron analogy[4-6] and the parton pair production.[7] The first one is a generalization of the fact that the photon can interact with hadrons like another hadron (vector meson) and the second one follows from the parton models that the two photons can create a parton pair which subsequently annihilate into hadrons. The difference in these two mechanisms has been discussed in Ref. 7. Since the photons in reaction (1) are predominantly near their mass shells, the photon-hadron analogy part is believed to be more important and shall be discussed first.

Using the photon-hadron analogy and regge behavior, the cross section $\sigma_{\gamma\gamma \to \text{hadrons}}$ has been estimated by various authors.[4-6] Assuming that it is dominated by the pomeron and leading secondary trajectories, we have

$$\sigma_{\gamma\gamma \to \text{hadrons}}(s') = a + \frac{b}{\sqrt{s'}} + O\left(\frac{1}{s'}\right) \tag{4}$$

Substituting Eq. (4) into Eq. (3a), the total cross section can be analytically evaluated. First few leading terms of σ are

$$\sigma = \left(\frac{\alpha}{\pi}\right)^2 \left(\ell n \frac{E}{m_e}\right)^2 \left\{ a\left[\left(\ell n \frac{s}{s_0}\right)^3 - 3\,\ell n \frac{s}{s_0} + \frac{35}{8} + \cdots\right] + \frac{b}{\sqrt{s_0}}\left[4\,\ell n \frac{s}{s_0} + 2 + \cdots\right] + O\left(\frac{s}{s_0}\right) \right. \tag{5}$$

Notice that, since the photon spectra are peaked at low values of s', the integrated cross section in Eqs. (3) and (5) receives substantial contribution from s' near s_0. Hence the contributions from the secondary trajectories are suppressed relative to that from the pomeron by a factor of $s_0^{-1/2}\ \ell n(s/s_0)^{-1}$ instead of $s^{-1/2}$. Similarly, contributions from the correction terms in Eq. (4) are relatively suppressed by a factor of $s_0^{-1}\ [\ell n(s/s_0)]^{-2}$. The cross section is dominated by the pomeron only in the case of a very large cut off energy, s_0, or at very high energies such that $s_0^{1/2}\ \ell n(s/s_0) >> 1$ GeV.

Using factorization, SU(3), and measured values of the nucleon-nucleon and nucleon Compton (γp) scattering cross sections, it has been estimated in Ref. 6 that

$$a = 0.24\,\mu b, \qquad b = 0.27\,\mu\text{b-GeV}. \tag{6}$$

With these values for a and b, σ is plotted in Fig. 2 as a function of E for several values of s_0. At high energies, σ should behave like $\left(\ell n \frac{E}{m_e}\right)^2 \left(\ell n \frac{s}{s_0}\right)^2$ but it increases much faster with E at lower energies. Higher order electromagnetic processes asymptotically can contribute to σ with higher powers of $\ln(s/s_0)$ but are negligible for the present consideration.[5]

Observing a total cross section comparable to the prediction of a particular model is hardly sufficient to verify the model. Therefore, we must study some other features of the hadron production as predicted by the regge model. Certain features of the hadron distributions in reaction (1) can be readily discussed from Eqs. (3) and (4) without invoking the details of the single hadron inclusive spectra. A few of them are the total invariant mass, energy, momentum, and multiplicity distributions of the hadrons. The average invariant mass is given by

$$< \sqrt{s'} > \simeq \frac{1}{\sigma} \left(\frac{\alpha}{\pi}\right)^2 \left(\ln \frac{E}{m_e}\right)^2 \int_{s_0}^{s} \frac{ds'}{s'^{1/2}} \left[\frac{1}{2}\left(2 + \frac{s'}{s}\right)^2 \ln\left(\frac{s}{s'}\right) - \left(1 - \frac{s'}{s}\right)\left(3 + \frac{s'}{s}\right)\right]$$

$$\times \quad \sigma_{\gamma\gamma \to \mathrm{hadrons}}(s')$$

$$= \frac{1}{\sigma} \left(\frac{\alpha}{\pi}\right)^2 \left(\ln \frac{E}{m_e}\right)^2 \left\{ a \left[\left(4 + \frac{2}{9} + \frac{12}{25}\right) s^{1/2} - 4 s_0^{1/2} \ln \frac{s}{s_0} + \cdots\right]\right.$$

$$\left. + \, b \left[\left(\ln \frac{s}{s_0}\right)^2 - 3 \ln \frac{s}{s_0} + \cdots\right] + O\left(\frac{1}{s_0^{1/2}} \ln \frac{s}{s_0}\right)\right\} , \qquad (7)$$

which asymptotically behaves like $s^{1/2} / [\ln(s/s_0)]^2$. Notice that, while both the pomeron and secondary trajectories can contribute comparable amounts to σ, only the former contributes in the high s' region. As a result, $< \sqrt{s'} >$ is more sensitive to the pomeron contribution. It should also be obvious that if a cut off, s_0, is imposed on s', $< \sqrt{s'}>$ will depend on s_0. In general, the average value is somewhere between 1 to 2 GeV for 1.5 GeV $\leq$ E $\leq$ 4.5 GeV, as illustrated in Fig. 3a.

In each event from reaction (1), the hadronic system should have a net longitudinal momentum in the e^-e^- cm frame, since in general the two virtual photons are not emitted with equal and opposite momenta. According to the photon spectra and the cross section $\sigma_{\gamma\gamma\to\text{hadrons}}$, this momentum distribution is given by

$$\frac{d\sigma}{d\omega_-} = 2\left(\frac{\alpha}{\pi}\right)^2 \left(\ell n\ \frac{E}{m_e}\right)^2 \frac{1}{E^4} \int_{(\omega_-^2+s_0)^{1/2}}^{2E-\omega_-} \frac{d\omega_+}{\omega_+^2-\omega_-^2} \left\{E^2+\left[E-\frac{1}{2}(\omega_++\omega_-)\right]^2\right\}$$
$$\times \left\{E^2+\left[E-\frac{1}{2}(\omega_+-\omega_-)\right]^2\right\} \sigma_{\gamma\gamma\to\text{hadrons}}\ (\omega_+^2-\omega_-^2)\ , \qquad (8)$$

where $\omega_- = \omega_1 - \omega_2$ is the total momentum of the hadrons in the e^-e^- cm frame and $\omega_+ = \omega_1 + \omega_2$ is the total energy. Substituting Eq. (4) into Eq. (8), the momentum distribution can be analytically evaluated. Although neither the final state lepton nor the total hadron (including neutrals) momentum can be easily measured, a checking of the total observable hadron momentum against Eq. (8) can still give us some qualitative feeling about the role of this particular mechanism in reaction (1). In Fig. 3b, we have plotted the average magnitude of ω_-, $<|\omega_-|>$, as a function of E. It increases with E and behaves like $E/\ell n(s/s_0)$ at high energies. For E between 1.5 GeV and 4.5 GeV, $<|\omega_-|>$ varies from 0.5 GeV to 1.5 GeV and therefore sizable net momentum should be observed. Due to this fact, the total energy of the hadron, ω_+, is always greater than the total invariant mass, $\sqrt{s'}$. The energy distribution also can be obtained from Eq. (8) by the simple substitution $\omega_+ \longleftrightarrow \omega_-$ and appropriate change of the integration limits. The average value of the total energy, $<\omega_+>$, is plotted in Fig. 3c. It is comparable with E which is half of the total e^-e^- cm energy, at lower energies, becomes approximately half of E at higher energies, and increases like $E/\ell n(s/s_0)$ asymptotically.

Although the average hadron multiplicity, $<n>$, can not be obtained from Eqs. (3) and (4) alone, it is also possible to obtain without knowing much details of the hadron spectra. It has been observed in purely hadronic reactions[8] and γp scattering[9] that the average multiplicity for a given hadron, $\bar{n}_h$, increases logarithmically with total energy s. According to the Mueller Regge analysis,[10] $\bar{n}(s)$ is given by

$$\bar{n}_h(s) = c_h \ln s + d_h + O(s^{-1/2}) \tag{9}$$

and c_h is independent of the initial particles if the pomeron is a factorizable simple pole. Such behavior is approximately exhibited by the data in Refs. 8 and 9. In Ref. 9, we have

$$c_{\pi^-} = 0.44 \pm 0.04 \ , \qquad c_{\text{charged}} = 0.93 \pm 0.12 \ . \tag{10}$$

Using the photon-hadron analogy, the average multiplicity in the subprocess (2) at any s' should also be given by Eqs. (9) and (10) and the average multiplicity in reaction (1) is then given by

$$\begin{aligned} <n> &\simeq \frac{1}{\sigma} \left(\frac{\alpha}{\pi}\right)^2 \left(\ln \frac{E}{m_e}\right)^2 \int_{s_0}^{s} \frac{ds'}{s'} \left[\frac{1}{2}\left(2 + \frac{s'}{s}\right)^2 \ln \frac{s}{s'} - \left(1 - \frac{s'}{s}\right)\left(3 + \frac{s'}{s}\right)\right] \\ &\times \left[c_h \ln s' + d_s + O\left(\frac{1}{\sqrt{s'}}\right)\right] \sigma_{\gamma\gamma \to \text{hadrons}}(s') \\ &= \frac{2}{3} c_h \ln \frac{s}{s_0} + \text{constant} + O\left(\frac{1}{\ln(s/s_0)}\right) + O\left(\frac{1}{s_0^{1/2} \ln(s/s_0)}\right) . \end{aligned} \tag{11}$$

From Eq. (11), we can see that $<n>$ also increases as $\ln s$ but at a rate different from that in $\bar{n}$. The constant term can not be determined without additional information about the contributions of the secondary trajectories to the hadron spectra. The correction terms are different from those in Eq. (9). The terms of the order of $1/\ln(s/s_0)$ represents the effects of the next leading terms in σ and can be easily calculated. The last term arises from the correction terms in Eq. (9) and the fact that substantial contribution to the cross sections come from low values of s' near s_0.

The single hadron inclusive distributions have hardly been discussed for reaction (1) and its subprocess (2). As seen from Ref. 9, Feynman scaling is a reasonably good approximation in γp scattering even at relatively low energies and the inclusive distribution in the proton fragmentation region is qualitatively in agreement with that in other hadronic reactions. These features are expected from the Mueller-Regge analysis and the photon-hadron analogy. When such ideas are generalized to the subprocess (2), the inclusive distributions in reaction (1) can be related to those from γp reactions in the central and photon fragmentation regions. For a given type of hadron h, we have

$$
\begin{aligned}
f_h^{\gamma\gamma}(x^*, p_\perp^*) &\equiv p_0^* \left.\frac{d^3\sigma(x^*, p_\perp^*)}{dp_\parallel^* \, d^2 p_\perp^*}\right|_{\gamma\gamma \to h + \text{anything}} \\
&= \frac{\sigma_{\gamma\gamma \to \text{hadrons}}}{\sigma_{\gamma p}} \, p_0^* \left.\frac{d^3\sigma(|x^*|, p_\perp^*)}{dp_\parallel^* \, d^2 p_\perp^*}\right|_{\gamma p \to h + \text{anything}} \\
&\equiv \frac{\sigma_{\gamma\gamma \to \text{hadrons}}}{\sigma_{\gamma p}} \, f_h^{\gamma p}(|x^*|, p_\perp^*)
\end{aligned} \tag{12}
$$

where p_0^*, $p_\parallel^*$, and $p_\perp^*$ are respectively the time, longitudinal, and transverse components of the final state hadron momentum, $x^* = 2p_\parallel^*/\sqrt{s'}$ is the Feynman scaling variable, $|x^*| > 0$ denotes the photon fragmentation region in γp scattering and σ is the total cross section. Since the $\gamma\gamma$ cm frame can not be determined if neither the final state electrons nor the energies and momentum of all the hadrons, including neutrals, are measured in reaction (1), it is not suitable to use the kinematical variables in this frame. In colliding beam experiments, the final state hadron momenta can be easily measured in the e^-e^- frame, which are related to those in the $\gamma\gamma$ cm frame by

$$p_0^* = p_0 \cosh\alpha + p_{\parallel} \sinh\alpha$$

$$p_{\parallel}^* = p_0 \sinh\alpha + p_{\parallel} \cosh\alpha$$

$$p_{\perp}^* = p_{\parallel} \,, \tag{13}$$

where

$$\cosh\alpha = \frac{\omega_1 + \omega_2}{\sqrt{4\omega_1\omega_2}} \,, \qquad \sinh\alpha = \frac{\omega_1 - \omega_2}{\sqrt{4\omega_1\omega_2}} \,. \tag{14}$$

Thus the single hadron inclusive distribution in reaction (1) is given by

$$p_0 \frac{d^3\sigma(E, p_{\parallel}, p_{\perp})}{dp_{\parallel}\, d^2p_{\perp}} \simeq \left(\frac{\alpha}{\pi}\right)^2 \left(\ell n \frac{E}{m_e}\right)^2 \frac{1}{E^4} \int \frac{d\omega_1}{\omega_1} \frac{d\omega_2}{\omega_2} \left[E^2 + (E-\omega_1)^2\right] \left[(E^2 + (E-\omega_2)^2\right]$$

$$\times\ \theta(1 - x_0^*)\ f_h^{\gamma\gamma}(x^*, p_{\perp}) \,, \tag{15}$$

where $x_0^* = 2p_0^*/\sqrt{s'}$ and x^* are given by Eqs. (13) and (14) in terms of $p_{\parallel}$, $p_{\perp}$, ω_1, and ω_2. The θ-function is the energy conservation constraint in the sub-process (2). Strictly speaking, Eqs. (12) and (15) are valid only at very high energies, while the $\gamma\gamma$ cm energy is always very low in reaction (1) for e^-e^- energies available in the near future. However, since the deviations from Feynman scaling in hadronic and γp reactions are small and the energy dependence in $\sigma_{\gamma\gamma}$ and $\sigma_{\gamma p}$ tend to cancel each other, Eqs. (11) and (14) may be useful for estimating the inclusive distributions to within 30% for a reasonable cut off like $s_0 \simeq 1\ \mathrm{GeV}^2$.

To obtain some quantitative feeling of the inclusive distribution, we can approximately parametrize the right hand side of Eq. (12), by

$$f_{\pi^-}^{\gamma p}(x^*, p_\perp) \simeq 26\,\pi\, e^{-1.47 x^{*2} - 7.6\, p_\perp^2}\ \mu b/\mathrm{GeV}^2, \quad x^* > 0 \ . \tag{16}$$

A comparison of Eq. (16) with the data is shown in Figs. 4 and 5. Obviously, this parameterization is too simple to accurately describe data. In particular, the correlation between the x^*-dependence and $p_\perp$-dependence is neglected and the peak near $x^* = 1$ is not reproduced in Eq. (16). The peak is predominantly due to the pions decay from the "elastic" ρ production, $\gamma + p \to \rho^0 + p$. In reaction (1), there also can be such a peak due to the pions decay from the "elastic" process, $\gamma + \gamma \to \rho^0 + \rho^0$. However, this peak will not be present for $\sqrt{s'} \lesssim 1.5$ GeV and, for $\sqrt{s'}$ above this energy, will be smoothed out in the e^-e^- cm frame by integrating over the $\gamma\gamma$ cm energy and momentum. Because of these over simplified approximations, we want to stress that Eq. (16) is used only as a rough estimation of the hadron distribution.

We can also introduce the Feynman scaling variable $x = p_\parallel / E$ for the inclusive distribution (15). Although neither will this distribution exhibit scaling nor will the total cross section for reaction (1) reach a constant, it can be shown that if $f_h^{\gamma\gamma}$ scales, $f_h^{e^-e^-}(E, p_\parallel, p_\perp)/\sigma$ exhibits Feynman scaling at $x = 0$ and behaves like $(\ln s/s_0)^{-1}$, for $0 < x < 1$. This behavior is illustrated in Fig. 6. Notice that the x-dependence is quite different from that in Eq. (16), simply because of the momentum spread of the $\gamma\gamma$ cm frame and the sharp fall off of of the photon spectra in s'. The angular dependence of the inclusive spectrum also can be studied from Eqs. (18),(15) and (16). Since the cut off in $p_\perp$ is typically 0.3 GeV/c and not much smaller than the total available energy, there should be very little effect of this cut off. Substantial fraction of the hadrons can be produced at finite angles even the electrons are scattered forward relative to the beam.

So far, we have only discussed the contribution to the cross sections from one particular mechanism, namely, the Regge contribution to the even C hadron states from the two photon process with the photon-hadron analogy. There are some other features of photons being quite different from the hadrons. For example, gauge invariance requires a local interaction, the seagull term, between the photons and scalar particles. This type of interaction is unique to the photons and can not be related to hadronic reactions by factorization. In the parton models, such local interaction for the production of a hadron pair can take place via a parton loop, as illustrated in Fig. 1b. The local interaction between the two photons arises from the seagull diagrams for scalar partons and the z-graphs in the time ordered perturbation theory for spin 1/2 partons.[11] More generally, multi-hadron productions via the creation and subsequent annihilation of a parton pair,[7] can not be taken into account by the photon-hadron analogy. The effects of the parton pair annihilation and its difference from the photon-hadron analogy have been extensively discussed in Ref. 7 for reaction (2). From light cone arguments, the parton annihilation contribution to reaction (2) is given by the absorptive part of the parton loop diagram,[12] as shown in Fig. 1c, for high values of the photon masses and s'. If we simply use this diagram for all values of photon masses and s' to estimate the contribution, it turns out to be very small compared with σ_T in Eq. (2). Possibilities for such parton pair annihilation mechanism to be important are discussed later.

Besides the hadronic states, with even C, the ones with odd C can also be produced in e^-e^- scattering. The most important mechanism for the latter is shown in Fig. 1d, where a massive time-like photon is emitted from one of the electrons and subsequently decay into hadrons. The spectrum of this virtual photon can be calculated from quantum electrodynamics and the hadron spectra from the decay of the virtual photon can be obtained from the inclusive spectra in e^+e^- reactions, if the latter is indeed dominated by the single photon annihilation. Estimates of such contributions for various exclusive states has been worked out.[13] As seen from Ref. 13, the contribution is important only when one of the electrons is detected at wide angles and is small compared with reaction (2) as far as the total cross section is concerned. Detailed contribution to the total and inclusive cross sections are being estimated.[14]

In view of the relatively large cross section observed in e^+e^- reactions and its discrepancy with the parton model predictions, we shall discuss some of their consequences to the e^-e^- scattering. The parton model describes the e^+e^- annihilation by the diagram shown in Fig. 7a. At high energies, the total cross section is given by the absorption part of the parton loop diagram shown in Fig. 7b and can be written as

$$\sigma_{e^+e^- \to \text{hadrons}} = \left(\frac{4\pi\alpha^2}{3s}\right) N, \tag{17}$$

where $N = \sum_{j=\frac{1}{2}} Q_j^2 + \frac{1}{4} \sum_{j=0} Q_j^2$ and Q_j is the charge of each parton with spin j. Possible mechanisms for the cross section to deviate from Eq. (17) can be attributed mainly to zero, one, or two photon processes.

For the possibility of the zero photon processes, it implies that the leptons can directly interact with hadrons. Depending on the details of the models for such interactions, the e^-e^- cross sections may or may not be affected. For example, take the simplest model in which the e^+e^- cross section is given by the scattering of two geometrical objects, as motivated by the apparent constancy of $\sigma_{e^+e^- \to \text{hadrons}}$, then so would be the e^-e^- cross section. Since the former is much larger than the estimate given by Eq. (3), a substantial deviation from this equation should be observed. On the other hand, more complicated models can make a certain mechanism enhanced in one reaction and suppressed in another. If the e^+e^- reaction can be mediated by a meson which directly couple to e^+e^- with a strength of the order of α and strongly decay into observed hadrons, than the single virtual meson annihilation contribution to $\sigma_{e^+e^- \to \text{hadrons}}$ can be at least comparable to the one given by Eq. (17). On the other hand, although this meson can also mediate e^-e^- scattering via a process like the two photon process, its contribution can be suppressed relative to the one in Eqs. (2) and (3) by two factors of the meson propagators for a massive meson.

If the observed e^+e^- cross section is indeed due to the one photon process, then it is necessary to consider contributions other than the one given by Eq. (17). One such possibility, within the parton models, is simply that the parton loop diagram is not a good approximation at present energies, where the parton fragmentation regions can overlap and therefore the cross section is not given by an incoherent sum as in Eq. (17). If this is the case, the parton annihilation contribution to reaction (2) also can not be estimated by the loop diagram alone and it is interesting to see if this contribution can become comparable to the photon-hadron analogy part. A second possibility, also for the parton model, is the presence of the parton form factors.[15] In the model of Ref. 15, the effects of the form factors are enhanced only for the very virtual photons and therefore will not contribute to reaction (2). Yet another possibility for the one photon process is the presence of some $J = 1$, odd C, high mass, broad near the available e^+e^- energies. It would be interesting to see if there are also such resonances in the even C channels. But due to the fact that s' is much smaller than s, high mass resonances can hardly be produced in e^-e^- collisions.

The possibility of the two photon process being responsible for the observed e^+e^- cross sections trivially have direct implications on reaction (2). As seen from our esitmates, such cases would require certain "anomalous" behavior in the two photon process itself in order to produce a large cross section.

To conclude, we have estimated the Regge contribution to the total and single hadron inclusive cross sections and the energy, momentum, and multiplicity distributions in reaction (2). Whether there will be substantial deviations from our estimates would discriminate certain classes of models for the e^+e^- reaction. If such a deviation is present, then a much better understanding for the e^-e^-, as well as e^+e^-, reaction should be needed.

The author wishes to thank P. Zerwas for interesting discussions.

REFERENCES

1. For a review of the two photon process, see H. Terazawa, Rev. of Mod. Phys. 45, 615 (1973).
2. A. Litke, et al., Phys. Rev. Letters 30, 1189 (1973). Talk given by H. Newan, published in the Proceedings of Summer Institute on Particle Physics, Vol. I, 255, Stanford Linear Accelerator Center Report No. SLAC-167 (1973).
3. K. F. Weizsäker, Z. Physik 88, 612 (1934) and E. J. Williams, Phys. Rev. 45, 729 (1934), R. H. Daliz and D. R. Yennie, Phys. Rev. 105, 1598 (1951).
4. R. W. Brown and I. J. Muzinich, Phys. Rev. D4, 1496 (1971).
5. S. J. Brodsky, J. Kinoshita, and H. Terazawa, Phys. Rev. D4, 1532 (1971).
6. Talk given by J. Rosner, published in ISABELLE Physics Prospects, BNL-17522 (1972).
7. See, for example, T. F. Walsh, talk given at the International Colliquium on Photon-Photon Collision in Electron-Positron Storage Rings (1973).
8. See, for example, W. Frazer et al., Rev. Mod. Phys. 44, 284 (1972).
9. K. C. Moffeit et al., Phys. Rev. D5, 1603 (1972).
10. A. H. Mueller, Phys. Rev. D8, 2936 (1970).
11. S. J. Brodsky, F. E. Close and J. F. Gunion, Phys. Rev. D6, 177 (1972).
12. H. Terazawa, Phys. Rev. D5, 2259 (1972).
13. J. Parisi, Talk given at the International Colloquium of Photon-Photon Collisions in Electron-Positron Storage Rings, Paris (1973).
14. Work in progress with P. Zerwas.
15. G. B. West, Stanford University preprint ITP-454-Stanford (1974).

FIGURE CAPTIONS

1. (a) Dominant two-photon contribution to the hadron production in e^-e^- scattering, where the shaded area represents a general $\gamma\gamma$ hadrons vertex.

   (b) Hadron production from two-photons via a parton loop, where the lines labelled by q and $\bar{q}$ represent the parton pair.

   (c) High energy, large photon mass limit of the parton model. The dashed line represents where the absorptive part is taken.

   (d) Some diagrams for the production of hadrons with odd C in e^-e^- scattering.

2. Total hadron production cross sections given by Eqs. (3), (4) and (6).

3. (a) The average value of s' given by Eq. (9).

   (b) The average net momentum of the hadrons in the e^-e^- cm frame given by Eq. (8).

   (c) The average total hadron energy in the e^-e^- cm frame.

4. Comparison of the x-dependence between Eq. (16) and the data of Ref. 9 for $\gamma p \to \pi^- +$ anything, where the solid line is given by Eq. (16) and $0 < x < 1$ is the photon fragmentation region.

5. Comparison of the $p_\perp$-dependence similar to that in Fig. 4.

6. Behavior of the normalized invariant cross section for π^--production as a function of the scaling variable in the e^-e^- cm frame.

7. (a) Hadron production via a parton pair in the single photon annihilation process.

   (b) High energy behavior of the parton model. The dashed line indicates where the absorptive part is taken.

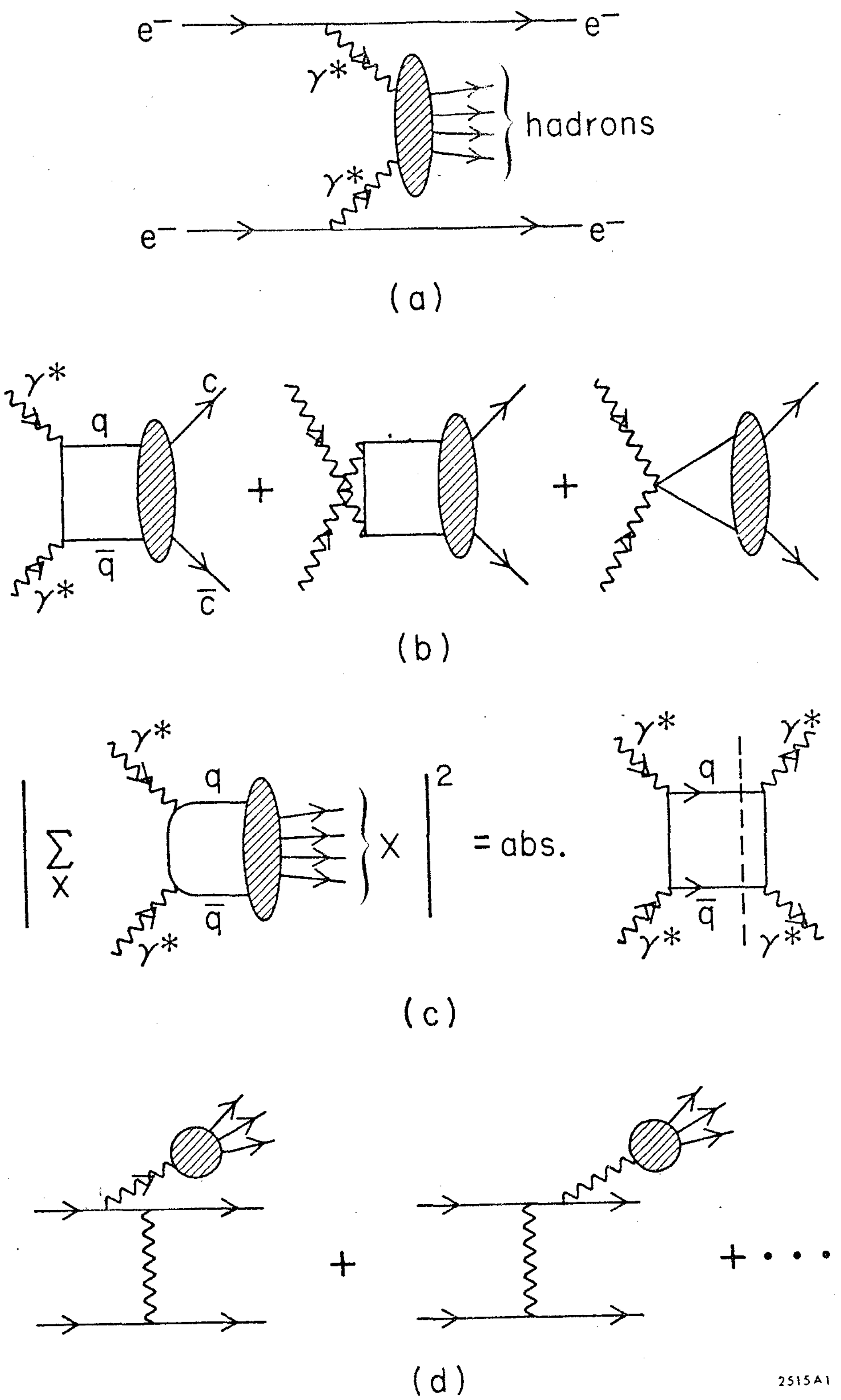

Fig. 1

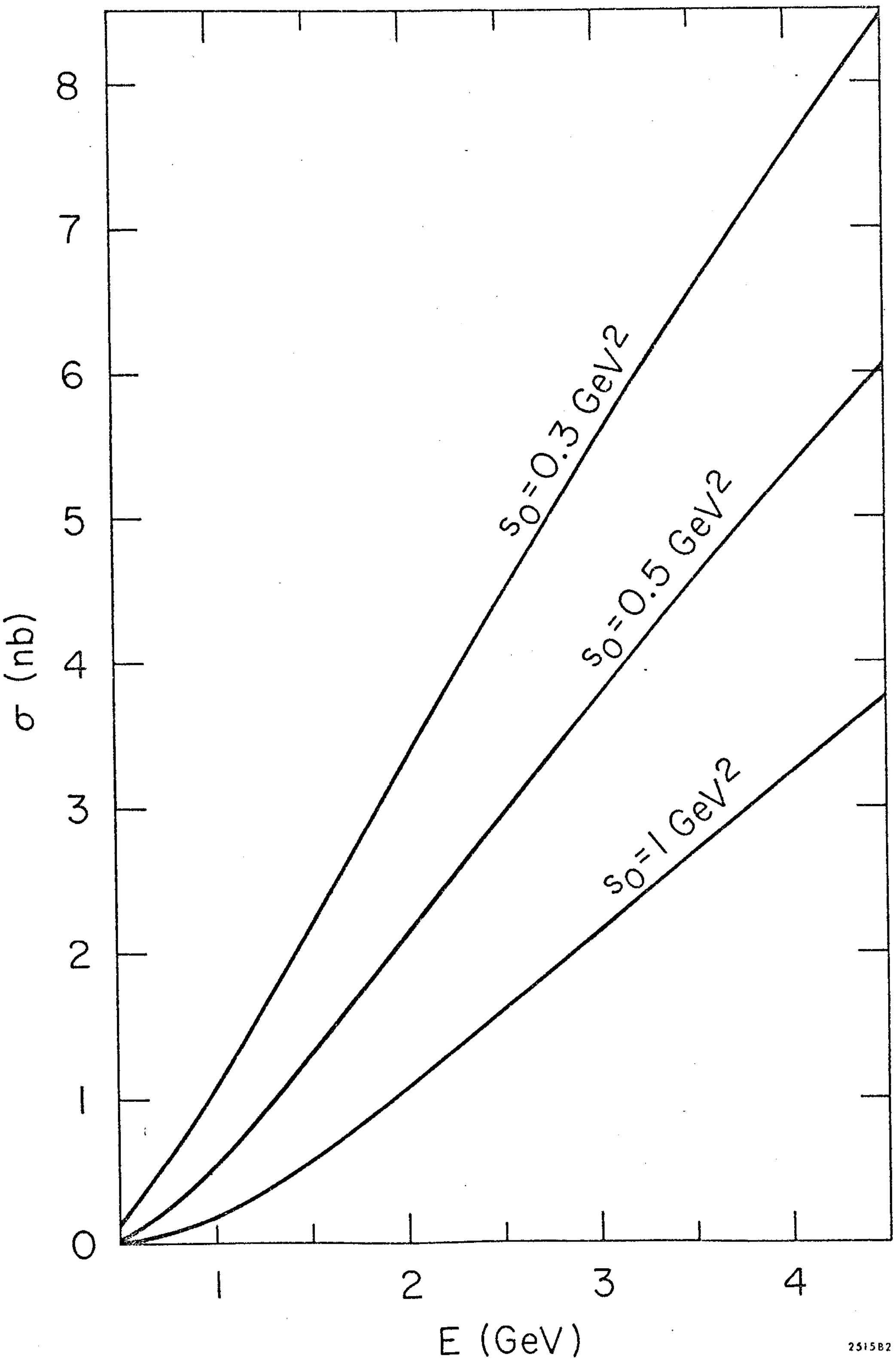

Fig. 2

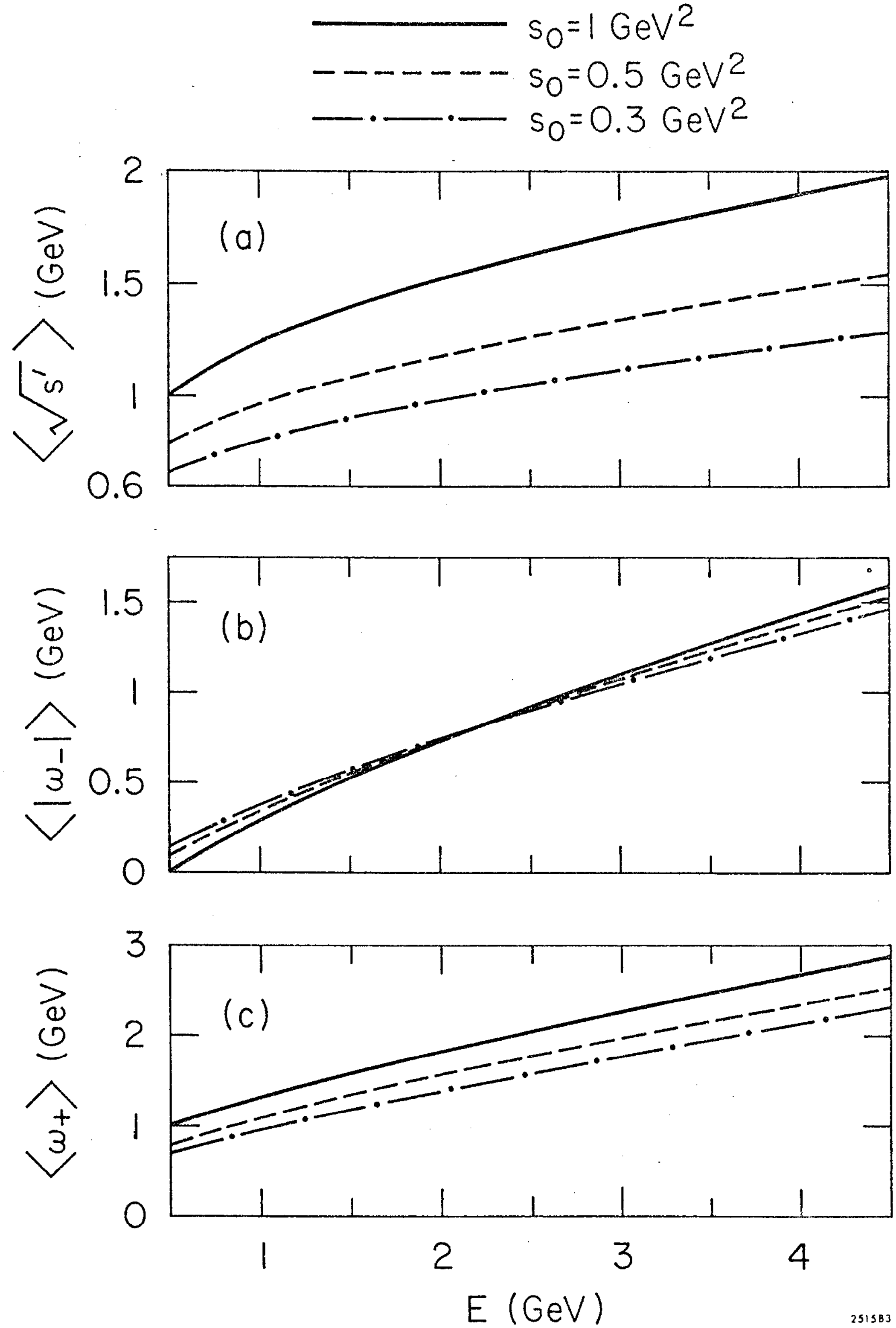

$s_0=1\ GeV^2$
$s_0=0.5\ GeV^2$
$s_0=0.3\ GeV^2$
(a)
$\langle\sqrt{s'}\rangle$ (GeV)
2
1.5
1
0.6
(b)
$\langle|\omega_-|\rangle$ (GeV)
1.5
1
0.5
0
(c)
$\langle\omega_+\rangle$ (GeV)
3
2
1
0
1
2
3
4
E (GeV)
251583

Fig. 3

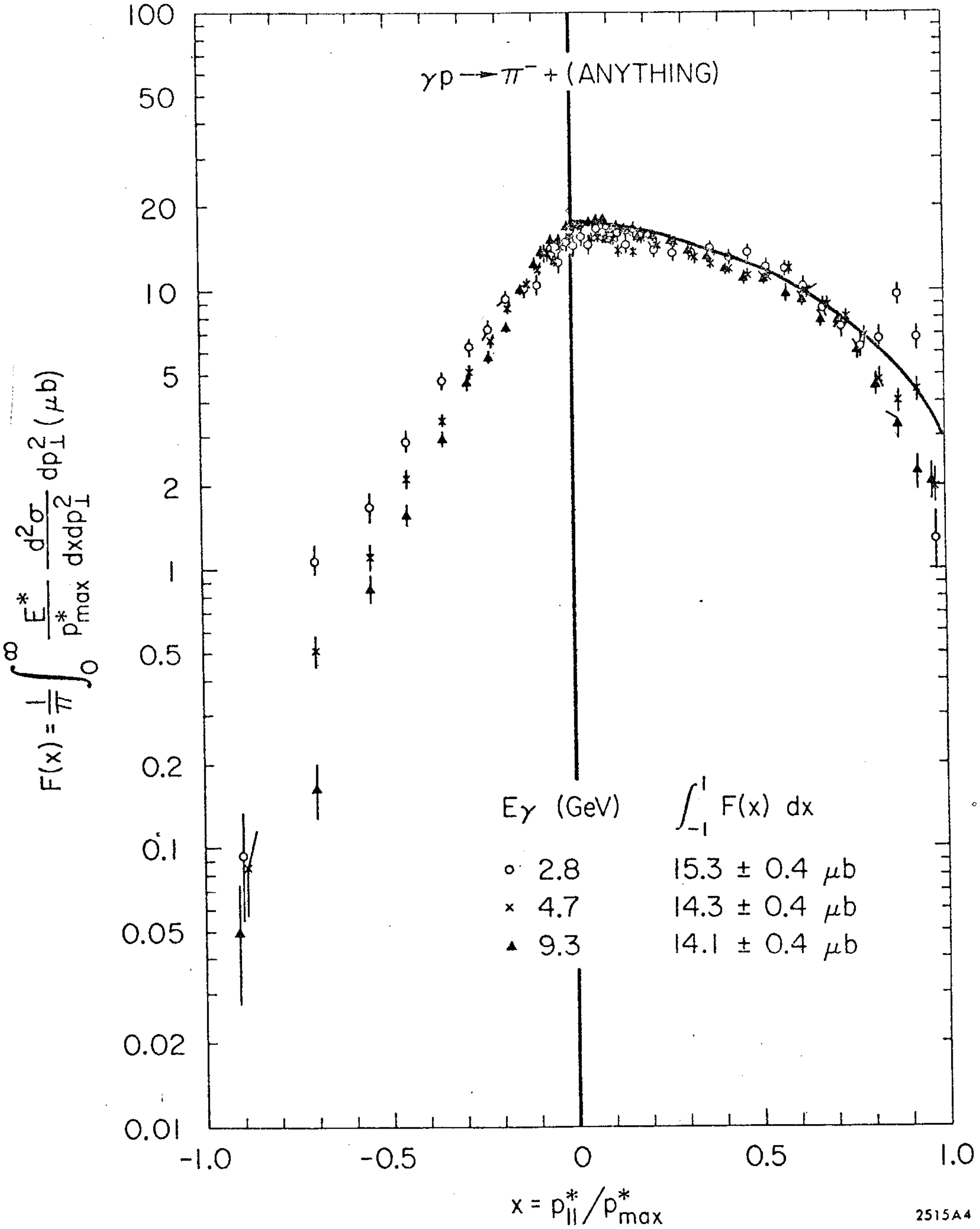

$\gamma p \rightarrow \pi^- + $ (ANYTHING)
$F(x) = \frac{1}{\pi}\int_0^\infty \frac{E^*}{p^*_{max}} \frac{d^2\sigma}{dx dp_\perp^2} dp_\perp^2$ (μb)
$x = p^*_{\parallel}/p^*_{max}$
Eγ (GeV)
$\int_{-1}^{1}$ F(x) dx
2.8
15.3 ± 0.4 μb
4.7
14.3 ± 0.4 μb
9.3
14.1 ± 0.4 μb
2515A4

Fig. 4

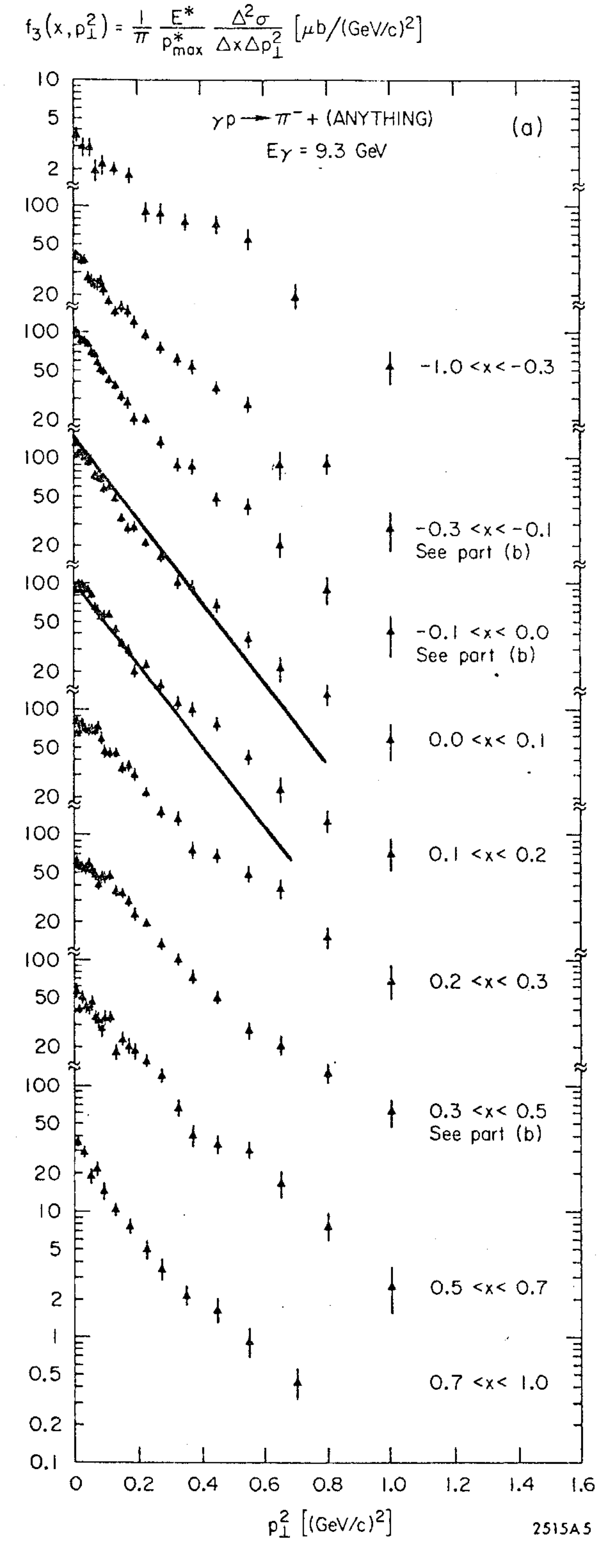

$f_3(x, p_\perp^2) = \frac{1}{\pi} \frac{E^*}{p^*_{max}} \frac{\Delta^2\sigma}{\Delta x \Delta p_\perp^2}$ [μb/(GeV/c)^2]
$\gamma p \to \pi^- +$ (ANYTHING)
$E\gamma$ = 9.3 GeV
(a)
$-1.0 < x < -0.3$
$-0.3 < x < -0.1$
See part (b)
$-0.1 < x < 0.0$
See part (b)
$0.0 < x < 0.1$
$0.1 < x < 0.2$
$0.2 < x < 0.3$
$0.3 < x < 0.5$
See part (b)
$0.5 < x < 0.7$
$0.7 < x < 1.0$
$p_\perp^2$ [(GeV/c)^2]
2515A5

Fig. 5

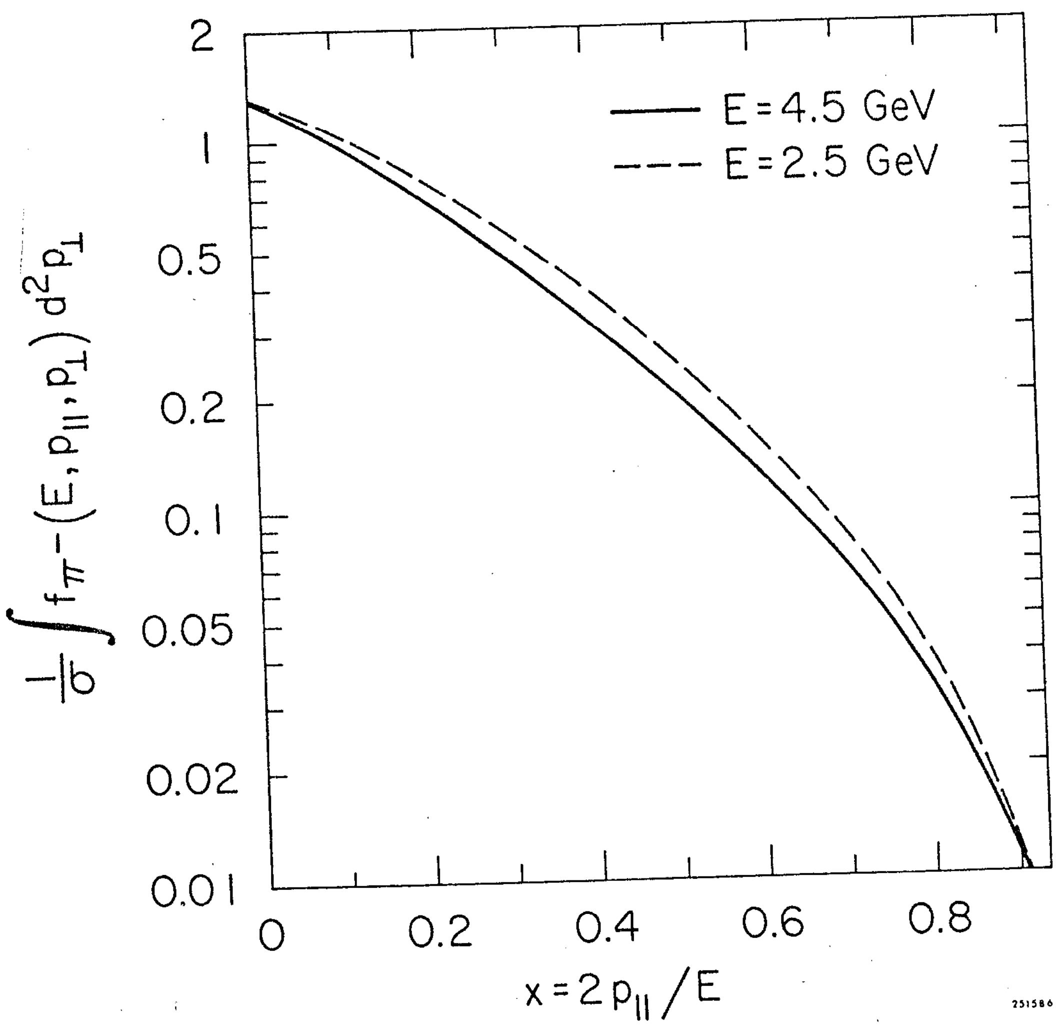

E = 4.5 GeV
E = 2.5 GeV
$\frac{1}{\sigma}\int f_{\pi^-}(E, p_{\parallel}, p_{\perp})\, d^2p_{\perp}$
2
1
0.5
0.2
0.1
0.05
0.02
0.01
0
0.2
0.4
0.6
0.8
$x = 2p_{\parallel}/E$
251586

Fig. 6

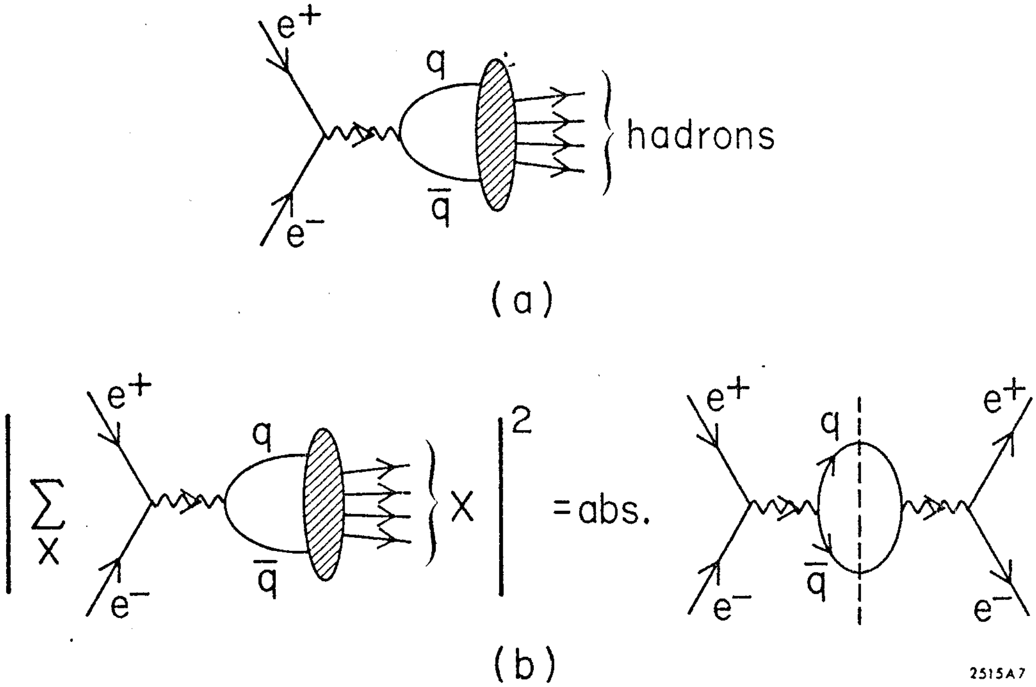

Fig. 7